Electrochemical Insertion of Lithium into Polyacrylonitrile-Based Disordered Carbons

Yongju Jung,[a] Min Chul Suh,[a] Hwashim Lee,[b] Myungsoo Kim,*[b] Sang-Ick Lee,[a]
Sang Chul Shim,[a] and Juhyoun Kwak[a]

[a]Department of Chemistry, Korea Advanced Institute of Science and Technology, 373-1 Kusung-Dong, Yusung-Gu,
Taejon 305-701, South Korea
[b]Division of Chemistry and Radiation, Korea Research Institute of Standards and Science, Yusung-Gu,
Taejon 305-600, South Korea

ABSTRACT

Electrochemical lithium insertion into polyacrylonitrile (PAN)-based disordered carbons was studied using the techniques of discharge/charge tests, cyclic voltammetry, and ^{7}Li nuclear magnetic resonance (NMR) spectroscopy. The PAN-based carbons were prepared by vacuum pyrolysis of PAN at 500, 800, and 1000°C. They showed charge capacities between 254 and 380 mAh/g in the first cycle. ^{7}Li NMR spectra showed two kinds of lithium insertion sites in the PAN-based carbons: a reversible site where lithium is removed in the subsequent charge process and an irreversible site where lithium remains intact. The NMR results suggest that lithium in fully Li-inserted PAN-based carbons has an ionic character, and reversible site lithium resides between negatively charged carbon layers.

Introduction

Numerous studies on the electrochemical insertion of lithium into various carbon materials have been reported.[1-8] Such intensive research has resulted from the recognition that carbons are promising as anode materials for lithium-ion batteries.[3,8] Studies on lithium intercalation into graphite, in particular, have been well established.[1,6,7,9-12] It is known that a maximum of one lithium atom per six carbon atoms can be intercalated when lithium is fully intercalated into graphite. In LiC$_6$, the intercalated lithium exists as a screened ion between two adjacent graphite layers, the theoretical specific capacity of LiC$_6$ being 372 mAh/g.

Recently, there have been numerous reports on lithium insertion into disordered carbons prepared by pyrolysis of organic precursors below 1000°C.[3,4,8,14] In general, these carbons show higher capacities than those of graphite. These high capacities and structures of the disordered carbons prepared at low temperatures suggest that there should be a mechanism different from that of graphite for lithium insertion. Lithium insertion into the disordered carbons with high capacities showed two kinds of electrochemical behavior. First, the carbon materials composed of single graphene sheets predominantly have voltage profiles which show little hysteresis and a low-voltage plateau.[14-18] Dahn proposed that lithium can be adsorbed on both of the surfaces of these single graphene sheets.[14,16] In this case, the theoretical maximum capacity is 740 mAh/g, which corresponds to $x = 2$ in Li$_x$C$_6$. Second, the carbon materials containing much hydrogen show voltage profiles with large hysteresis.[3,4,8,14] Several mechanisms have been proposed to explain both the high capacity and the large hysteresis which are generally observed during the lithium insertion in carbons having significant quantities of hydrogen.[8,14,19,20]

Recently, Dahn pointed out mistakes of both mechanisms suggested by Mabuchi et al.[8] and by Sato et al.[19] and proposed a new mechanism of lithium insertion where the inserted lithium binds to a carbon atom which also binds a hydrogen atom, causing a change in the bonding orbital for the carbon-carbon bond from sp^2 to sp^3.[14,20]

Many disordered carbons prepared from organic precursors have been found to be promising anode materials for lithium-ion batteries. However, there have been only a few reports about the electrochemical behavior of PAN-based carbons, which have been found to be inappropriate for electrode materials due to poor reversible capacity.[21-24] Recently, Verbrugge and Koch reported that PAN-based carbon fibers may be useful negative electrodes for lithium-ion batteries through cyclic voltammetric (CV) analysis.[25] Nevertheless, the electrochemical characteristics of PAN-based carbons have not been clearly identified, and there have been no studies on the effect of pyrolysis temperature (T_p) upon the electrochemical behavior of PAN-based carbons. In this study, we report lithium insertion into PAN-based disordered carbons prepared by pyrolysis of PAN at various temperatures to evaluate the effect of pyrolysis temperature (T_p) on the electrochemical characteristics of PAN-based carbons and to give insight into a mechanism of lithium insertion into PAN-based carbons.

Experimental

The PAN-based disordered carbons were prepared from PAN (Taekwang Industrial Co., Ltd, Korea) by vacuum pyrolysis at temperatures of 500, 800, and 1000°C, denoted as PAN-500, PAN-800, and PAN-1000, respectively. The vacuum pyrolysis technique used in this study is described elsewhere.[26] These samples were ground to a fine carbon powder with particle size of less than 100 μm using ball mills. The x-ray diffractometry (XRD) was carried out on
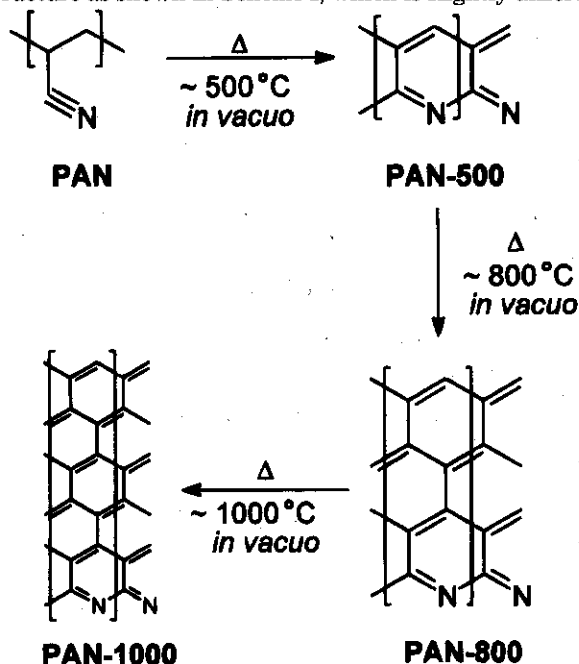
* Electrochemical Society Active Member.

a Rigaku x-ray diffractometer (Rigaku D/MAX-RC 12 kW system) with Cu K_α radiation. The data were collected from 10 to 100° in scattering angle (2θ). The average crystallite sizes along the a axes (L_a) were estimated from the (100) diffraction peak using the Scherrer equation.[27] Elemental analysis was carried out using an elemental analyzer from Foss Heraeus Analysentechnik Instrument.

The PAN-based carbons were mixed with 7 weight percent (w/o) of poly(tetrafluoroethylene) binder in isopropyl alcohol. The resulting mixtures were deposited on SUS-EXMET (stainless steel expanded metal grids) and pressed to form a thin electrode with thickness of 300 to 350 μm. After the carbon electrodes were cured for 3 h at 280°C, they were repressed, dried under vacuum for 24 h at 150°C, and stored in an argon-filled glove box to avoid exposure to air. Electrochemical measurements were performed in a three-electrode cell made of polypropylene at ambient temperature. The organic electrolyte used was 1.0 M LiPF$_6$ in ethylene carbonate (EC)/1,2-dimethylcarbonate (DMC) (2/1, v/v) solution (battery grade, Mitsubishi Petrochemical Co., Ltd.). A large amount of solution was always used to get rid of the influence of compositional change of the electrolyte. Lithium metal was used as a counter and a reference electrode. The surface area of the counterelectrode was about three times larger than that of the carbon electrode. The cyclic voltammetry of the carbon electrodes was carried out in the range 0 to 3 V $vs.$ Li/Li$^+$ at scan rates of 1 mV/s. The discharge (inserting lithium) and charge (removing lithium) tests for the carbon electrodes were carried out between 0 and 2.5 V $vs.$ Li/Li$^+$ using constant currents of 24.8 mA/g. Fully Li-inserted carbons and fully Li-removed carbons in the first cycle were made by discharging to 0 V and by subsequent charging to 2.5 V after the first discharging, respectively. The fully Li-inserted carbons and the fully Li-removed carbons after the full lithium insertion in the first cycle were examined by ^{7}Li NMR spectroscopy (Bruker AM-300; resonance frequency 116.6 MHz). A solution of 1 M LiCl/D$_2$O was used as an external standard.

Results and Discussion

Structure and composition of PAN-based carbons.— Elemental analysis of the PAN-based carbons (Table I) shows the atomic ratio of hydrogen to carbon (H/C) to decrease from 0.34 to 0.06 with an increase of pyrolysis temperature (T_p). The atomic ratio of nitrogen to carbon (N/C) slowly decreases from 0.23 to 0.10 as T_p is increased. The results suggest that the PAN-based carbons have a structure as shown in Scheme I, which is slightly different

Table I. Results of elemental analysis and L_a values calculated from XRD patterns using the Scherrer equation.

Sample	T_p (°C)	L_a(Å)	Weight percentage (w/o)			Atomic ratio (a/o)	
			C	H	N	H/C	N/C
PAN-500	500	27	74.9	2.10	20.5	0.34	0.23
PAN-800	800	30	81.9	0.85	13.7	0.12	0.14
PAN-1000	1000	38	88.6	0.43	9.9	0.06	0.10

from that described elsewhere.[28] Scheme I shows that small-size carbon layers composed of aromatic rings are formed by the aromatization of PAN at low T_p, and the size of carbon layers becomes larger through condensation of aromatic rings as T_p is raised. It has been reported that the residual hydrogen and nitrogen are completely removed above 1000 and 1500°C, respectively.[28-30] The suggested structure of PAN-500, however, is not fully consistent with the results of the elemental analysis, because carbons having defect sites can be formed as shown in Scheme II.
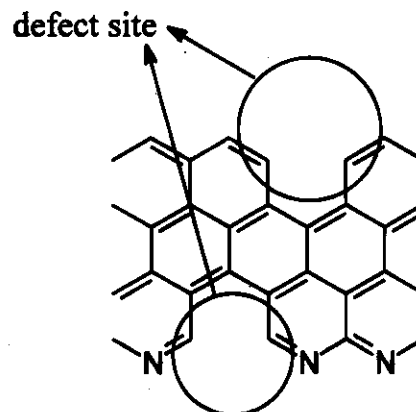
Scheme II. Structure with defect site in PAN-500.

Scheme I. Plausible structures of the PAN-based carbons prepared by vacuum pyrolysis of PAN.
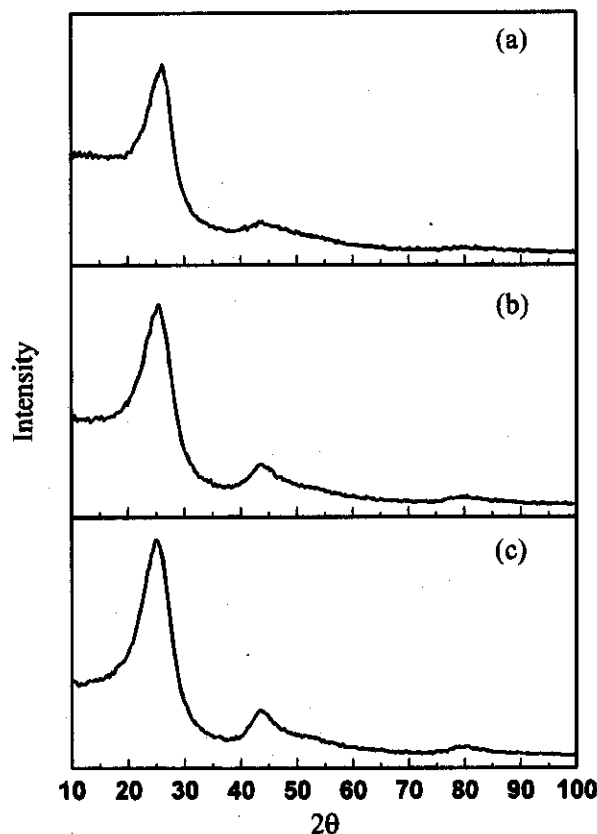

Fig. 1. XRD patterns of the PAN-based carbons: (a) PAN-500, (b) PAN-800, and (c) PAN-1000.

XRD patterns of the PAN-based carbons are shown in Fig. 1. All the peaks have broad shapes indicating highly disordered carbons.[31] The (002) and (004) peaks due to the stacking of carbon layers and the (100) and (110) peaks due to in-plane order are observed. The (002), (004), (100), and (110) peaks are observed at 2θ of near 25, 54, 44, and 80°, respectively. Figure 1 shows that the (002) and (100) peaks become sharp as T_p is raised from 500 to 1000°C. In PAN-500, a typical XRD pattern of disordered carbons is also observed. This is good evidence that the carbon layers are well stacked even at 500°C. The average crystallite sizes along the a axes (L_a) are estimated from the (100) diffraction peak using the Scherrer equation[27] and are shown in Table I. The approximate L_a values increase from 27 Å in PAN-500 to 38 Å in PAN-1000.

Electrochemical studies on the PAN-based carbons.— Figure 2 shows the discharge and charge curves of the PAN-based carbons during the first two cycles. The results of the discharge and charge tests of the three samples are summarized in Table II. As T_p is increased from 500 to 1000°C, the charge capacities of the PAN-based carbons decrease from 380 to 254 mAh/g in the first cycle. In all the PAN-based carbons, the cycle efficiencies (Q_{ch}/Q_{dis}) of the first and the second cycle are above 50 and 90%, respectively. The discharge and charge curves in Fig. 2b and c show almost no hysteresis; the discharge and charge steps occur over essentially the same potential range. On the contrary, Fig. 2a displays a hysteresis effect; however, it seems to be due to the overvoltages which arise from the low conductivity of PAN-500. In summary, the discharge/charge curves in Fig. 2, which were obtained between 0 and 2.5 V *vs.* Li/Li⁺, display typical curves for standard lithium insertion/removal processes in pyrolyzed carbons, where $x \le 1$ in Li_xC_6. Note that the curves in Fig. 2 do not show the hysteresis phenomenon occurring

Table II. Results of the charge/discharge tests for the PAN-based carbons.

Sample	Capacity (mAh/g)				Irreversible capacity (mAh/g)	Cycle efficiency (%)	
	Discharge		Charge				
	1st	2nd	1st	2nd		1st	2nd
PAN-500	731	389	380	362	351	52	93
PAN-800	605	341	340	338	265	56	99
PAN-1000	487	252	254	241	233	52	96

after reaching $x > 1$ in Li_xC_6, which is achieved only at potentials near bulk lithium deposition.[20]

The irreversible capacity usually observed in the first discharge cycle of carbon electrodes is defined as the difference in capacity between the first discharge and the subsequent charge. The PAN-based carbons tested in this study also show a large irreversible capacity. The irreversible capacities of the PAN-based carbons (Table II) decrease from 351 to 233 mAh/g as T_p is raised. This trend is similar to that observed in the recent work of Xing *et al.* in which they prepared carbons by pyrolysis of sugar.[32] Generally, it is accepted that the irreversible capacity is caused by the formation of a passivating film on the surface of the carbon electrodes due to the decomposition of electrolyte.[33]

Figure 3 shows reversible capacities and efficiency *vs.* cycle number for PAN-800. The cells were cycled between 0.0 and 2.5 V at a constant current density of 24.8 mA/g. Good efficiency is shown from the second cycle. At the tenth cycle, a high capacity of about 300 mAh/g is observed.

Figure 4 shows cyclic voltammograms (CV) of the PAN-based carbons. Upon the anodic scan, the charge (lithium removal) capacities are very low in the early cycles and gradually increase during repeated cycles. The low charge capacities observed in the early cycles indicate that a large amount of inserted lithium in the PAN-based carbons remains upon scan reversal. This is consistent with the results observed in the first cycle of discharge/charge tests. Higher anodic peak currents for the PAN-based carbons are observed in PAN-1000, compared with PAN-500 and PAN-800, indicating the kinetics of lithium insertion/re-
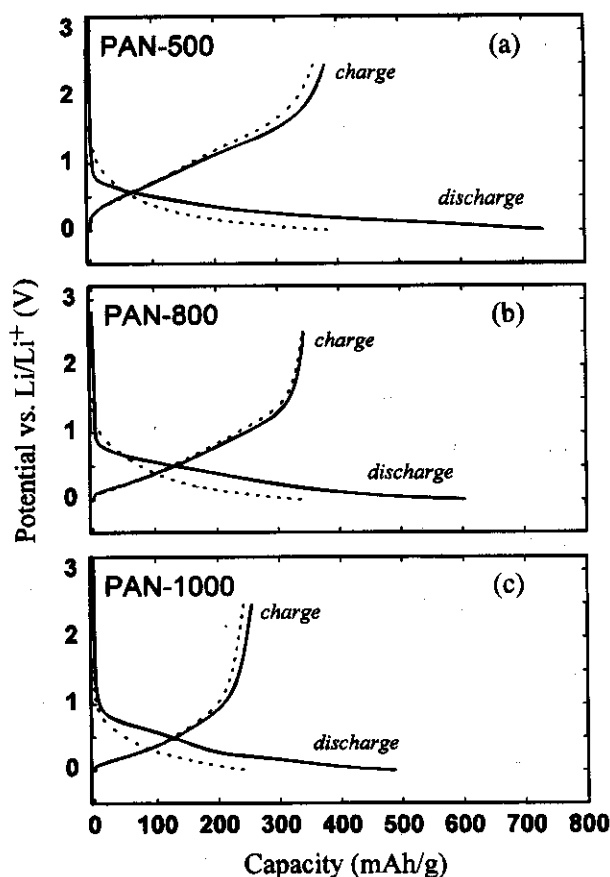
Fig. 2. Discharge/charge curves of the PAN-based carbons: (a) PAN-500, (b) PAN-800, and (c) PAN-1000. The solid and dot lines correspond to the first and second cycle, respectively.
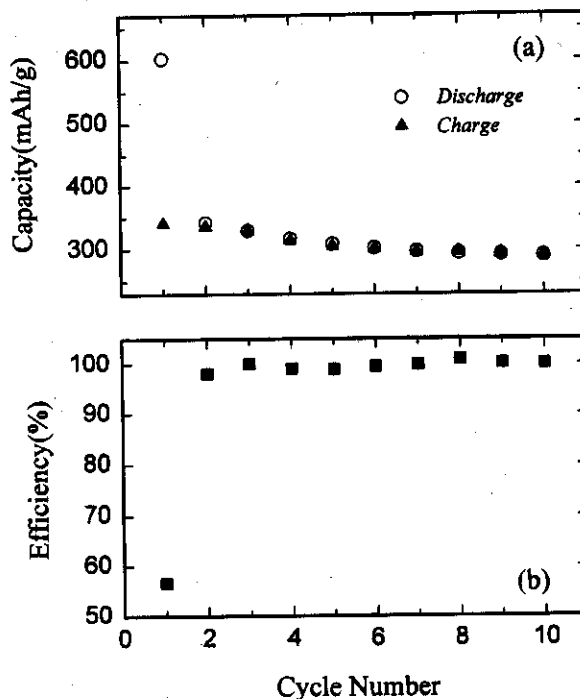
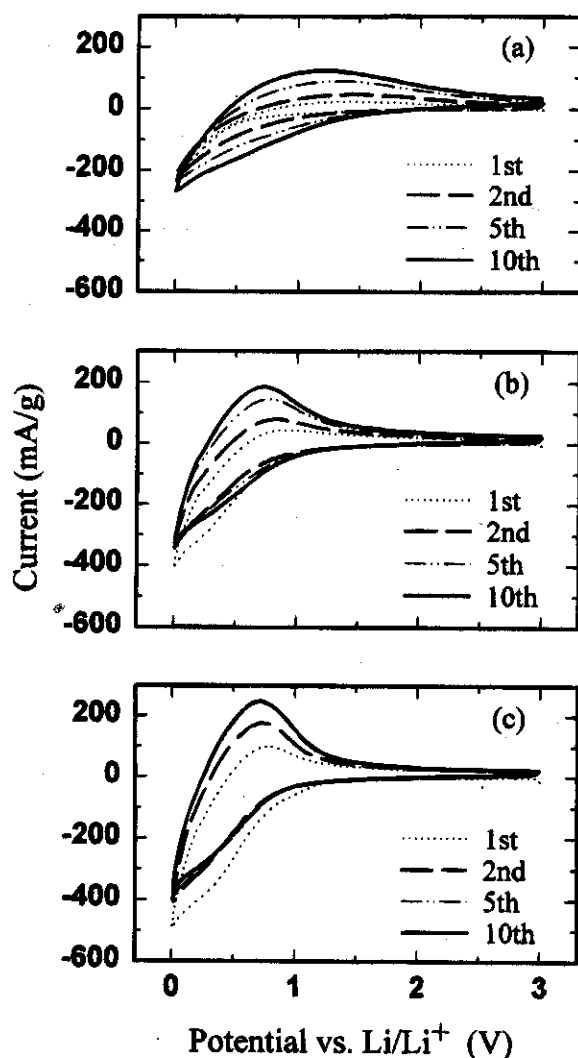Fig. 3. Plots of the capacity (a) and cycle efficiency (b) vs. cycle number in PAN-800.

Fig. 4. Cyclic voltammograms of the PAN-based carbons: (a) PAN-500, (b) PAN-800, and (c) PAN-1000.

Fig. 5. Plots of both discharge (Q_{dis}) and charge (Q_{ch}) capacities vs. cycle: (a) PAN-500, (b) PAN-800, and (c) PAN-1000.

moval in PAN-1000 to be the fastest among the three PAN-based carbons. It is probable that this feature is mainly due to better conductivity of PAN-1000 than those of PAN-500 and PAN-800. Discharge (lithium insertion) and charge (lithium removal) capacities are calculated in each cycle. The plots of both discharge capacities (Q_{dis}) and charge capacities (Q_{ch}) vs. cycle number are shown in Fig. 5. PAN-500 shows low values of Q_{dis} and Q_{ch} in the early cycles, compared with those of PAN-800 and PAN-1000 but similar values of Q_{dis} and Q_{ch} around the tenth cycle. The very low Q_{dis} and Q_{ch} of PAN-500 in the early cycles are attributed to the sweep rate being relatively fast compared to the kinetics of the lithium insertion/removal in PAN-500. It is believed in a fast potential sweep that lithium is not inserted into the deep inner parts of carbon particles in early cycles due to large ohmic (IR) drop, but into only the shallow inner parts of carbon particles. Thus, only shallow inner parts near the surface of carbon particles take in lithium from solution in early cycles. It is expected, however, that during repeated cycles, more and more lithium is inserted into the deep inner parts of carbon particles by solid-state diffusion. The plots of the cycle efficiency (Q_{ch}/Q_{dis}) vs. cycle are shown in Fig. 6. In the case of PAN-1000, Q_{ch}/Q_{dis} approaches almost unity in the tenth cycle. This observation proves that inserted lithium in PAN-1000 is completely removed upon scan reversal in the tenth cycle.

^{7}Li NMR spectra of the PAN-based carbons.—To investigate the lithium insertion sites and the chemical state of
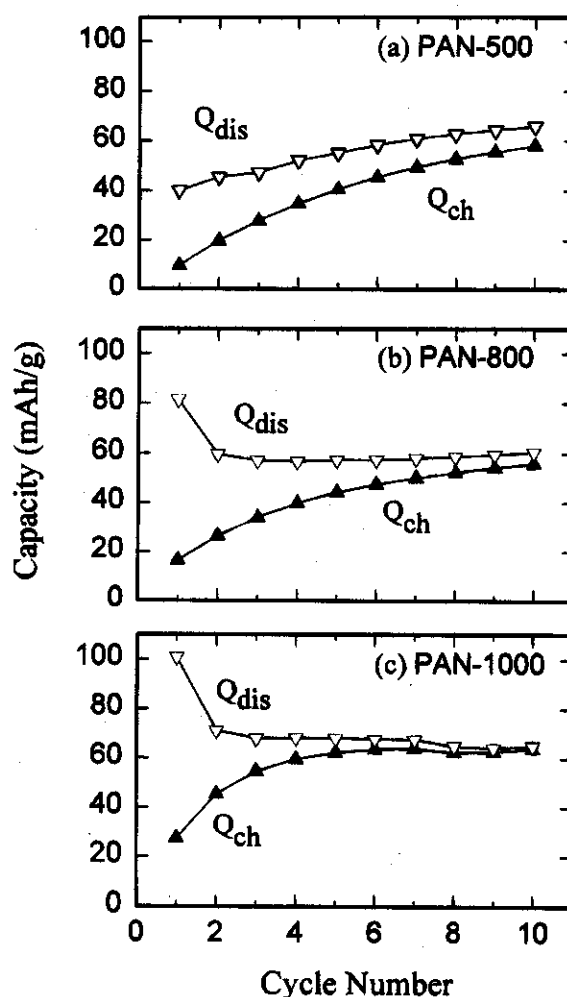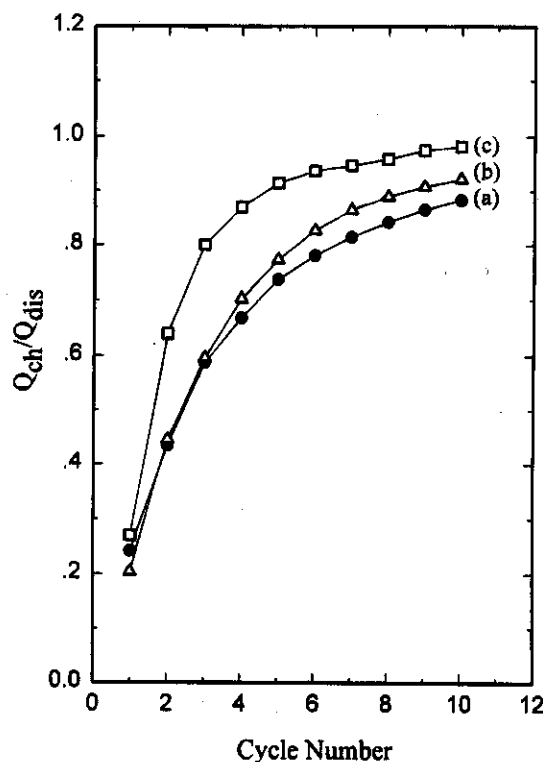

Fig. 6. Plot of Q_{ch}/Q_{dis} vs. cycle: (a) PAN-500, (b) PAN-800, and (c) PAN-1000.
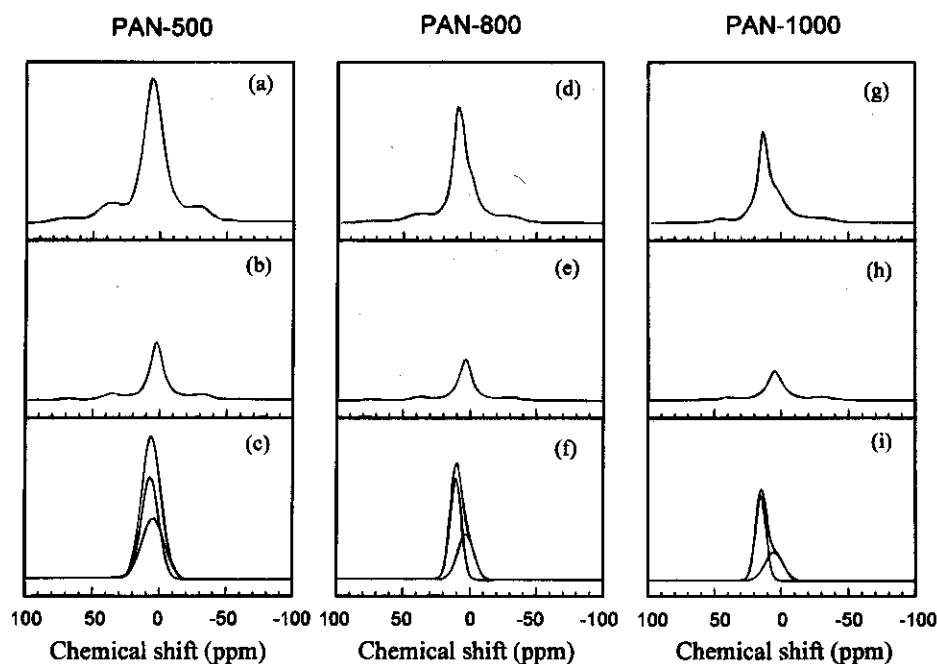
PAN-500   **PAN-800**   **PAN-1000**

Fig. 7. (a) , (d), and (g) are ^{7}Li NMR spectra of fully Li-inserted PAN-500, PAN-800, and PAN-1000, respectively. (b), (e), and (h) are ^{7}Li NMR spectra of fully Li-removed PAN-500, PAN-800, and PAN-1000, respectively. (c), (f), and (i) are the deconvoluted results for the main bands in PAN-500 (a), PAN-800 (d), and PAN-1000 (g), respectively.

lithium, ^{7}Li NMR spectra were obtained in both the fully Li-inserted PAN-based carbons and the fully Li-removed PAN-based carbons after the full lithium insertion in the first cycle (Fig. 7). The peaks for lithium in the fully Li-inserted PAN-500 (Fig. 7a), PAN-800 (Fig. 7d), and PAN-1000 (Fig. 7g) are observed at around 5, 10, and 14 ppm, respectively. The chemical shift of the fully Li-inserted PAN-based carbons increases with an increase of T_p. A similar trend was found in the recent work of Tatsumi et al. where they used mesocarbon microbeads (MCMBs) as electrode materials.[2] The peaks for lithium in the fully Li-removed PAN-500 (Fig. 7b), PAN-800 (Fig. 7e), and PAN-1000 (Fig. 7h) are observed at around 2, 3, and 5 ppm, respectively. The chemical shifts of lithium in the three PAN-based carbons are closer to that of LiCl (0 ppm) rather than that of metallic lithium (262 ppm), suggesting that lithium in the PAN-based carbons has an ionic character. The deconvoluted results for the peaks observed in the fully Li-inserted PAN-based carbons are shown in Fig. 7c, 7f, and 7i. The results indicate two kinds of lithium insertion sites: a reversible site where lithium is removed in the subsequent charge process and an irreversible site where lithium remains. The reversible peak due to the reversible site lithium is observed in the direction of downfield. On the other hand, the irreversible peak due to the irreversible site lithium is observed in the direction of upfield. It is suggested that the irreversible peak is caused by lithium salts in the passivating film.

The downfield shift of the reversible site lithium is observed with an increase of T_p as shown in Fig. 8. Such a downfield shift can be understood by a model where the lithium in the fully Li-inserted PAN-based carbons resides between negatively charged carbon layers. As T_p is raised, carbons with large condensed aromatic rings are formed, and the interlayer distance decreases. It is expected that the interactions between lithium ions and conduction electrons in the carbon plane are more favorable as the interlayer distance decreases, and the lithium in the PAN-based carbons prepared at higher T_p have a higher electron density. As a result, the chemical shift of lithium moves to downfield with an increase of T_p.

Conclusions

As T_p is increased from 500 to 1000°C, the charge capacities of PAN-based carbons decrease from 380 to 254 mAh/g in the first cycle. The discharge/charge curves of three PAN-based carbons, which were obtained between 0 and 2.5 V vs. Li/Li$^+$, show typical curves for standard

lithium insertion/removal processes in pyrolyzed carbons, where $x \leq 1$ in Li$_x$C$_6$. Higher anodic peak currents of the PAN-based carbons are observed in CV curves of PAN-1000, compared with those of PAN-500 and PAN-800. This feature indicates that the kinetics of the lithium insertion/removal in PAN-1000 are the fastest among the three PAN-based carbons. It is probable that this feature is mainly due to the higher conductivity of PAN-1000 compared to the other PAN-based carbons. ^{7}Li NMR spectra show two kinds of lithium insertion sites in the PAN-based carbons: a reversible site where lithium is removed in the subsequent charge process and an irreversible site where lithium remains.

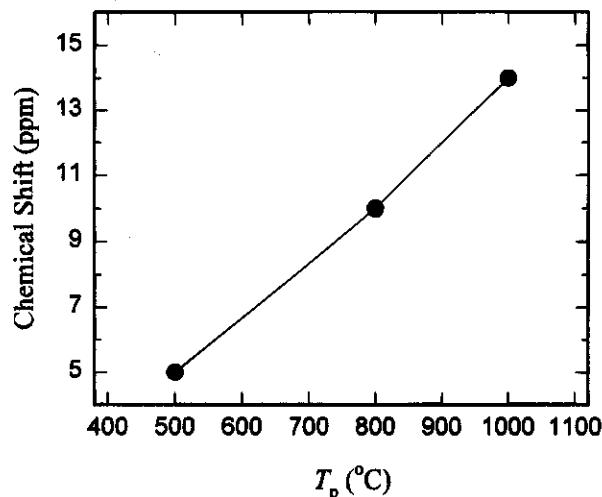Fig. 8. Plot of chemical shift of reversible site lithium vs. T_p.

REFERENCES

1. K. Tatsumi, N. Iwashita, H. Sakaede, H. Shioyama, S. Higuchi, A. Mabuchi, and H. Fujimoto, *This Journal*, **142**, 716 (1995).
2. K. Tatsumi, T. Akai, T. Imamura, K. Zaghib, N. Iwashita, S. Higuchi, and Y. Sawada, *ibid.*, **143**, 1923 (1996).
3. T. Zheng, Y. Liu, E. W. Fuller, S. Tseng, U. von Sacken, and J. R. Dahn, *ibid.*, **142**, 2581 (1995).
4. (a) S. Yata, H. Kinoshita, M. Komori, N. Ando, T. Kashiwamura, T. Harada, K. Tanaka, and T. Yamabe, *Synth. Met.*, **62**, 153 (1994); (b) S. Yata, Y. Hato, H. Kinoshita, N. Ando, A. Anekawa, T. Hashimoto, M. Yamaguchi, K. Tanaka, and T. Yamabe, *ibid.*, **73**, 273 (1995).
5. T. D. Tran, J. H. Feikert, X. Song, and K. Kinoshita, *This Journal*, **142**, 3297 (1995).
6. D. Aurbach and Y. Ein-Eli, *ibid.*, **142**, 1746 (1995).
7. T. Ohzuku, Y. Iwakoshi, and K. Sawai, *ibid.*, **140**, 2490 (1993).
8. A. Mabuchi, K. Tokumitsu, H. Fujimoto, and T. Kasuh, *ibid.*, **142**, 1041 (1995).
9. J. R. Dahn, R. Fong, and M. J. Spoon, *Phys. Rev. B*, **42**, 6424 (1990).
10. J. R. Dahn, *ibid.*, **44**, 9170 (1991).
11. T. Zheng, J. N. Reimers, and J. R. Dahn, *ibid.*, **51**, 734 (1995).
12. T. Zheng and J. R. Dahn, *Synth. Met.*, **73**, 1 (1995).
13. M. C. Suh and S. C. Shim, *Chem. Mater.*, **9**, 192 (1997).
14. J. R. Dahn, T. Zheng, Y. Liu, and J. S. Xue, *Science*, **270**, 590 (1995).
15. J. S. Xue and J. R. Dahn, *This Journal*, **142**, 3668 (1995).
16. Y. Liu, J. S. Xue, T. Zheng, and J. R. Dahn, *Carbon*, **34**, 193 (1996).
17. Y. Takahashi, J. Oishi, Y. Miki, M. Yoshimura, K. Shibahara, and H. Sakaomoto, Paper 2B05 in Extended Abstracts, p. 39, 35th Battery Symposium in Nagoya, Japan, Nov. 14-16, 1994.
18. N. Sonobe, M. Ishikawa, and T. Iwasaki, *ibid.*, Paper 2B09, p. 47.
19. K. Sato, M. Noguchi, A. Demachi, N. Oki, and M. Endo, *Science*, **264**, 556 (1994).
20. (a) T. Zheng, J. S. Xue, and J. R. Dahn, *Chem. Mater.*, **8**, 389 (1996); (b) T. Zheng, W. R. McKinnon, and J. R. Dahn, *This Journal*, **143**, 2137 (1996).
21. R. Kanno, Y. Takeda, T. Ichikawa, K. Nakanishi, and O. Yamamoto, *J. Power Sources*, **26**, 535 (1989).
22. N. Imanishi, S. Ohashi, T. Ichikawa, Y. Takeda, O. Yamamoto, and R. Kanno, *ibid.*, **39**, 185 (1992).
23. O. Chusid (Youngman), Y. Ein-Ely, and D. Aurbach, *ibid.*, **43-44**, 47 (1993).
24. R. Yazami, K. Zaghib, and M. Deschamps, *ibid.*, **52**, 55 (1994).
25. M. W. Verbrugge and B. J. Koch, *This Journal*, **143**, 24 (1996).
26. M. C. Suh and S. C. Shim, *Macromolecules*, **28**, 8707 (1995).
27. B. E. Warren, *Phys. Rev.*, **59**, 693 (1941).
28. J.-B. Donnet and R. C. Bansal, *Carbon Fibers*, Chap. 1-2, Marcel Dekker, New York (1990).
29. G. Savage, *Carbon-Carbon Composites*, Chap. 1-2, Chapman & Hall, London (1993).
30. P. L. Walker, Jr., *Chemistry and Physics of Carbon*, Vol 7, Marcel Dekker, New York (1971).
31. J. R. Dahn, A. K. Sleigh, H. Shi, J. N. Reimers, Q. Zhong, and B. M. Way, *Electrochim. Acta*, **38**, 1179 (1993).
32. W. Xing, J. S. Xue, and J. R. Dahn, *This Journal*, **143**, 3046 (1996).
33. R. Fong, U. von Sacken, and J. R. Dahn, *ibid.*, **137** 2009 (1990).